Building Engineering 2023; 1(1): 488.
Original Research Article

Dynamic vibration control of non-linear buildings using multiple tuned mass dampers

Hashim Ataie[1], Taiki Saito[2,*]

[1] *Graduate School of Engineering, Toyohashi University of Technology, Toyohashi 441−8580, Japan*

[2] *Department of Architecture and Civil Engineering, Toyohashi University of Technology, Toyohashi 441-8580, Japan*

*** Corresponding author:** Taiki Saito, saito.taiki.bv@tut.jp

ARTICLE INFO

Received: 15 November 2023
Accepted: 19 December 2023
Available online: 30 December 2023

doi: 10.59400/be.v1i1.488

Copyright © 2023 Author(s).

Building Engineering is published by Academic Publishing Pte. Ltd. This article is licensed under the Creative Commons Attribution License (CC BY 4.0). http://creativecommons.org/licenses/by/4.0/

ABSTRACT: In the field of civil engineering, tuned mass dampers (TMDs) serve as passive devices designed for dynamic vibration control of structures. When dealing with buildings exhibiting nonlinear behavior under dynamic loads, the effectiveness of TMDs may be affected by detuning due to the degradation of the building's strength. Therefore, addressing the non-linear behavior requires a unique strategy involving the tuning of TMDs to specific time periods following the onset of non-linearity. The proposed approach in this study entails a pushover analysis to establish the pushover capacity curve. The regions between the origin and a target drift of 1/150 are then represented using an idealized trilinear form, with the initial segment corresponding to linearity and subsequent segments capturing non-linear behavior. The second segment spans from the onset of non-linearity to a target drift of 1/400, and the third segment covers the drift range from 1/400 to 1/150. Examining this strategy involves calculating time periods for each segment. Subsequently, three single TMD (STMD) scenarios and one multiple TMDs (MTMDs) scenario with 3 TMDs, each tuned to time periods corresponding specific segments of the idealized trilinear, are compared in this study. The evaluation includes non-linear dynamic analysis of 7-story and 25-story reinforced concrete buildings equipped with these TMD scenarios. The floors maximum displacement and peak acceleration results indicate that the STMDs tuned to the time periods corresponding to the non-linear segments exhibit robustness, surpassing the performance of the STMD tuned to the fundamental period. Remarkably, the MTMD scenario, demonstrates superior robustness compared to all three STMD scenarios. Further analysis under wind load on the same 25-story building confirms the effectiveness of the MTMDs and STMD tuned to the nonlinearity segment compared to the STMD tuned to the fundamental period. This research provides valuable insights into TMD design for enhanced building performance under non-linear conditions.

KEYWORDS: dynamic vibration control; multiple tuned mass dampers; non-linear building; control strategy; pushover capacity curve; modal effective mass

1. Introduction

The application of TMDs for controlling the nonlinear behavior of buildings has been the focus of

attention in recent times. Numerous research efforts have been dedicated to investigating the efficacy of employing TMDs in addressing the challenges posed by nonlinear behaviors in buildings as the field of structural engineering continues to evolve. This reflects a growing interest in minimizing structural vibrations and enhancing overall stability.

Boccamazzo et al.[1] suggest employing a TMD featuring a spring exhibiting hysteretic behavior with pinching designed to regulate the response of nonlinear structures under seismic forces. The authors conduct two optimizations: The first involves stationary harmonic loading, and the second utilizes seismic records in the time domain, with both approaches yielding comparable results. In comparison to traditional TMDs, the newly proposed device exhibits increased resilience across various seismic intensities and greater efficacy in managing the nonlinear response of the primary structure. Huang et al.[2] propose employing a TMD with a restitutive force generated by an element made of shape memory alloy, allowing the device to prevent detuning through thermal control, consequently adjusting the frequency of the TMD. Lu et al.[3] investigates analytically and experimentally the application of a TMD in which the mass consists of particles colliding with each other, resulting in energy dissipation and a more resilient response compared to the conventional version.

Elias and Matsagar[4] conducted a thorough examination of the installation of multiple tuned vibration absorbers (MTVAs) positioned across both the height and plan of a building. Their primary objective was to mitigate the nonlinear behavior exhibited by the structure. Notably, they emphasized the importance of targeting the first few modes with a modal mass contribution of 90% or more, and all installed devices were conventionally tuned to the time period of each corresponding mode. The findings from their study revealed the efficacy of MTVAs when adhering to optimal placement criteria for multimode dynamic response control.

Domizio et al.[5] addressed potential stiffness and strength degradation during the control device's design. Their proposed TMD configurations include the classical single-degree-of-freedom TMD and the two-degree-of-freedom TMD with parallel and series arrangements, designed to control nonlinear responses in seismic scenarios. An objective function was introduced to sustain the control device's robustness against stiffness degradation. Calculations of the infinity norm of the frequency response magnitude were conducted for two stiffness reduction levels 75% and 50%, representing moderate and severe degradation in reinforced concrete structures. The results highlight that the configuration with two TMDs in series, tuned to 50% of the fundamental frequency of the healthy structure, demonstrated optimal effectiveness when the ductility demand exceeded 5. In short, numerous other studies have also been conducted to explore the application of TMDs in structures with non-linear behavior[6–9].

Distinguished from existing researches, this study introduces an innovative approach and specifically focuses on addressing non-linear behavior by tuning TMDs to specific time periods following the initiation of non-linearity. The proposed strategy involves a thorough process, beginning with a pushover analysis to derive the pushover capacity curve. Then it is transformed into a trilinear form covering a region between the origin and a target drift of 1/150. This form outlines the linearity and subsequent non-linear segments of the building's behavior. The tow nonlinear segments spans from the onset of non-linearity to a target drift of 1/400, and the drift range from 1/400 to 1/150. Following the calculation of the time periods corresponding to each segment, three STMD scenarios and one scenario featuring MTMDs with three TMD, each precisely tuned to those time periods, are subjected to comparison. Importantly, the total mass ratios of the MTMD scenario are equivalent to those of the STMD scenarios. The efficacy of these strategy is rigorously examined through non-linear dynamic analyses conducted on 7-story and 25-story RC buildings, utilizing frame models. The results,

encompassing floors' maximum displacement and peak acceleration, affirm the robustness of the STMDs tuned to the time periods corresponding to the non-linear segments, surpassing conventional STMD tuned to the fundamental period. Notably, the MTMD scenario exhibits superior robustness when compared to all three STMD scenarios. Furthermore, a comprehensive analysis under wind load conditions on the same 25-story building reaffirms the effectiveness of the MTMDs and STMD tuned to the nonlinearity segment compared to the STMD tuned to the fundamental period. This research contributes valuable insights into the TMD design to effectively mitigate the impact of non-linear behavior in buildings.

2. Control strategy

Traditionally, TMDs are designed to align with a building's fundamental period, with the goal of controlling its primary mode of vibration. As illustrated in **Figure 1**, the pushover capacity curve vividly illustrates the building's response. Notably, nonlinear behavior becomes apparent when the base shear force exceeds 733 kN resulting in a displacement of 0.8 cm at the top floor of this specific structure. Accordingly, during dynamic events like earthquakes and strong wind loads, buildings transition into a nonlinear range. In such circumstances, TMDs, initially tuned to the fundamental period, lose their efficacy. This is attributed to the building's diminishing stiffness as it yields, causing an increase in its period or decrease in its frequency. In response to this challenge, this study proposes an innovative approach: incorporating TMDs tuned to longer time periods than the fundamental period to effectively control non-linear buildings. The pushover capacity curve is idealized using a trilinear representation divided into three regions, as illustrated in **Figure 1**. The first region, denoted by segment $\overline{OA}$, signifies the linear range of the structure, while segments $\overline{AB}$ and $\overline{BC}$ represent the nonlinear segments covering a region between the onset of nonlinearity and a target drift of $1/150$. Rather than opting for a STMD tuned to the fundamental period, this research recommendation advocates for the installation of three smaller TMDs, each precisely tuned to the time periods corresponding to the stiffness characteristics of the three identified regions. This approach is proposed to enhance the overall effectiveness of the damping system and better address the dynamic response of the building throughout various stages of nonlinearity.

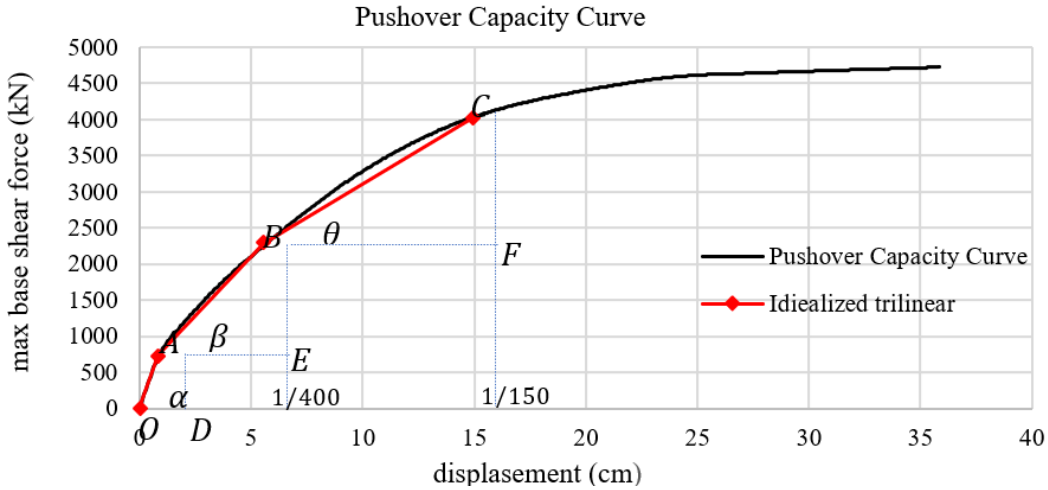

Figure 1. Illustration of an Idealized trilinear on pushover capacity curve of an RCC building in the X-direction.

As depicted in **Figure 1**, the stiffness of the building in regions $\overline{OA}$, $\overline{AB}$, and $\overline{BC}$ can be determined by taking the tangent of α, β and θ, respectively. A detailed step-by-step calculation procedure is outlined in **Table 1** for clarity and reference.

Table 1. Corresponding stiffness and time period calculation methods for each segment of the idealized trilinear.

Stiffness (K_i)	$T_i = 2\pi\sqrt{\frac{m_{eff}}{K_i}}$
$\tan\alpha = \overline{AD}/\overline{OD} = K_1$	T_1 (Fundamental period)
$\tan\beta = \overline{BE}/\overline{AE} = K_2$	T_2
$\tan\theta = \overline{CF}/\overline{BF} = K_3$	T_3

While m_{eff} represents the effective mass of the first dominant mode which is supposed to be controlled and calculated by the Equation (1)[10].

$$m_{eff} = \frac{(\emptyset^T M\zeta)^2}{\emptyset^T M\emptyset} \tag{1}$$

where $\emptyset$ is the mode shape, M is the mass matrix and ζ is a unit vector. It is noteworthy that the modeling and comprehensive analyses, including eigenvalue analysis, were conducted utilizing the STERA_3D software[10,11].

Tuning a STMD solely to the fundamental period of the building, corresponding to linear range, proves insufficient. Post-yielding, such a TMD would fall out of tune due to the diminishing strength of the structure. Therefore, in addition to conventional TMD, complementary TMDs, specifically tuned to the nonlinearity range of the building, become imperative. The introduction of these additional TMDs is crucial to address the evolving dynamic characteristics of the structure as it progresses from linear to nonlinear behavior, ensuring sustained efficacy in vibration control measures.

3. TMD optimal parameters

In this study, the optimal frequency ratios, and damping ratios of TMDs are calculated using the Equations (2) and (3), respectively[12].

$$f_i = \left(\frac{\sqrt{1-0.5\mu_i}}{1+\mu_i} + \sqrt{1-2\zeta_i^2} - 1\right) - \left[2.375 - 1.034\sqrt{\mu_i} - 0.426\mu_i\right]\zeta_i\sqrt{\mu_i} - \left(3.73 - 16.903\sqrt{\mu_i} - 20.496\mu_i\right)\zeta_i^2\sqrt{\mu_i} \tag{2}$$

$$\zeta_{d\,i} = \sqrt{\frac{3\mu_i}{8(1+\mu_i)(1-0.5\mu_i)}} + \left(0.151\zeta_i - 0.17\zeta_i^2\right) + \left(0.163\zeta_i + 4.98\zeta_i^2\right)\mu_i \tag{3}$$

where μ_i: Mass ratio of i^{th} TMD and ζ_i: Damping ratio of i^{th} mode.

Finally, the damping coefficient and stiffness of each TMD is calculated using Equations (5) and (6) respectively[13].

$$\omega_{di} = f_{opti}\omega_i \tag{4}$$

$$c_{di} = 2\zeta_{di}\omega_{di}m_{di} \tag{5}$$

$$k_{di} = \omega_{di}^2 m_{di} \tag{6}$$

4. Selected ground motion records (GMRs)

In this research, four distinct Ground Motion Records (GMRs) are selected to be applied in example buildings. These records span a moment magnitude scale ranging from 6.1 to 7.5 Mw and exhibit a focal depth variation between 6 and 66 km, details of which are comprehensively presented in **Table 2**[14,15].

Table 2. Detail of input earthquake ground motions.

No	Record name	location	Date (yy/mm/dd)	Depth (km)	Magnitude (Mw)	Duration (sec)	PGA (gal)	
							Component	PGA
1	El Centro	El Centro, California, USA	1940/05/19	8.8	6.9	53.8	East-West	210.1
							Up-Down	−206.3
2	Kobe	Kobe, Japan	1995/01/17	17	6.9	50	East-West	617.1
							Up-Down	332.2
3	Taft	Kern County, California, USA	1952/07/21	16	7.5	54.4	East-West	175.9
							Up-Down	102.9
4	Tohoku	Tohoku, Japan	1978/02/20	60	6.1	41	East-West	202.6
							Up-Down	153.0

The acceleration response spectrum of the selected GMRs is visually represented in **Figure 2**. It is established using the data obtained by ViewWave Software[16]. The numerical examples included in this study involve two reinforced concrete buildings: One with 7 stories and the other with 25 stories. These structures are characterized by restricted movement along the horizontal Y direction. Consequently, only the east-west and up-down components of the GMRs are applied to obtain dynamic response characteristics of the buildings under consideration.

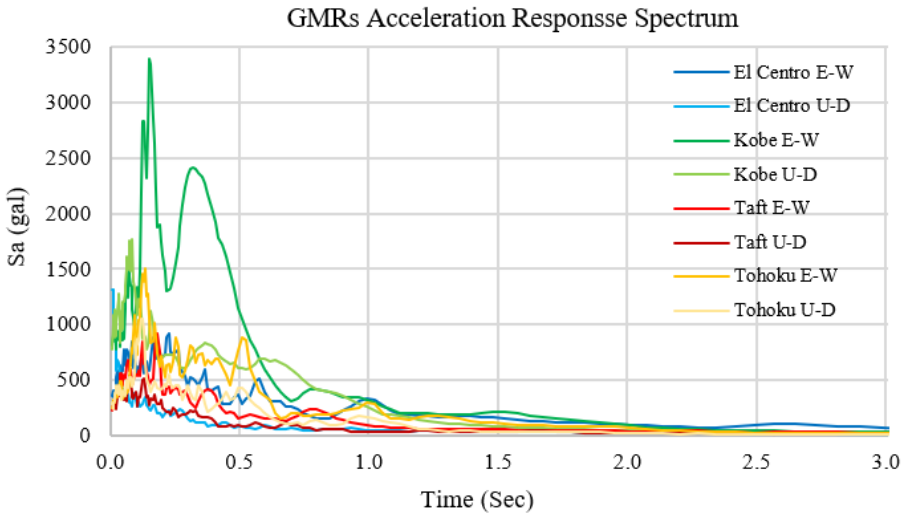

Figure 2. GMRs acceleration response spectrum (2% damping).

5. Numerical Example 1 (7-story building)

5.1. Model information and TMD design

A 7-story reinforced concrete building, depicted in both its 3D frame model and plan in **Figure 3**, is under consideration. The assumed load weight per unit is 12 $kN/m2$, resulting in a calculated weight of each story equaling 3.24×10^3 kN. The height of each story is set at 3200 mm. The building has no basement floor and the foundation structure is assumed to be sufficiently rigid, and the analysis assumes that the first-floor columns of the frame model are fixed to the foundation. The building's fundamental damping ratio is 0.02.

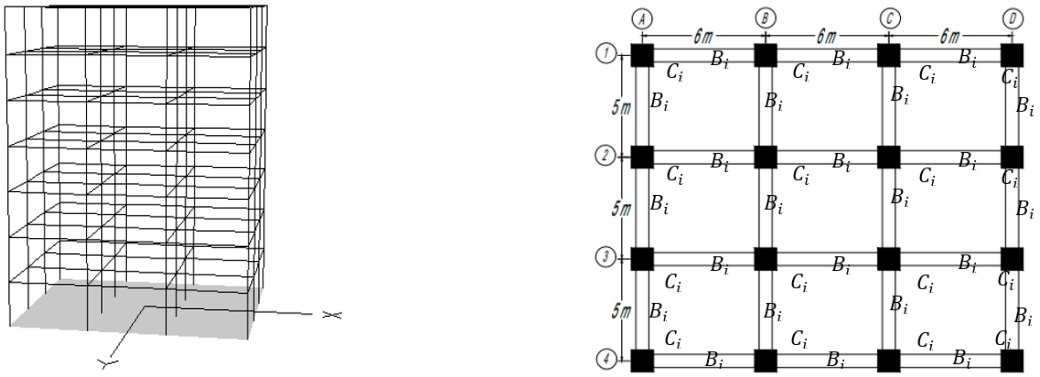

(a) frame model **(b)** Typical plan

Figure 3. 7-Story model.

For a more comprehensive understanding of the building's members, **Table 3** provides detailed information about the columns and beams.

Table 3. Element properties of 7-story building.

Floors	Members	$Dimensions\ (mm)$	Longitudinal rebars		$F_c(N/mm^2)$	$F_y(N/mm^2)$
1–2	C1	500 × 500	24 Ø25		24	390
3–7	C2	500 × 500	20 Ø25		24	390
1–2	B1	b = 400, h = 550	Top	5Ø22	24	390
			Bottom	5Ø22		
3–7	B2	b = 400, h = 550	Top	4Ø22	24	390
			Bottom	4Ø22		

By conducting pushover analysis of the non-controlled building, the pushover capacity curve is established as shown in **Figure 4**. Based in explanation in Section 2, the capacity curve is idealized by a trilinear which the segment $\overline{OA}$ represents the linear behavior of the building and segments $\overline{AB}$, and $\overline{BC}$ represents the nonlinear range of the building.

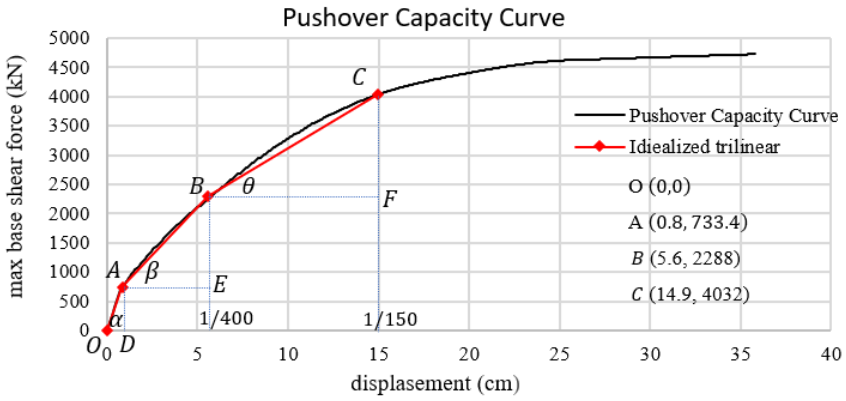

Figure 4. Illustration of Idealized trilinear on pushover capacity curve of 7-story building in the X-direction.

Furthermore, by conducting eigenvalue analysis, the mode shape of the first dominant mode will be derived. Consequently, sing Equation (1), the effective mass of the first mode is calculated to be 1.938 $kN.s^2/mm$. Referring to **Figure 3**, and considering the value of the first mode's effective mass, the three time periods are calculated as presented in **Table 4**.

Table 4. Time periods corresponding to three segments of idealized trilinear pushover capacity curve of 7-story building.

angle	Stiffness (K)	$K_i(^{kN}/_{cm})$	$T_i = 2\pi\sqrt{\frac{m_{eff}}{K_i}}$ (sec)	Hereinafter referred as
$\tan\alpha$	$K_1 = \overline{AD}/\overline{OD}$	$K_1 = 874.0$	$T_1 = 0.935$	Fund T
$\tan\beta$	$K_2 = \overline{BE}/\overline{AE}$	$K_2 = 328.6$	$T_2 = 1.526$	$N - LT_1$
$\tan\theta$	$K_3 = \overline{CF}/\overline{BF}$	$K_3 = 186.1$	$T_3 = 2.027$	$N - LT_2$

Taking into account the decided mass ratio (here, 3%) and utilizing Equations (2)–(6), the stiffness and damping coefficients for each TMD are computed, as outlined in **Table 5**.

Table 5. Parameter values and information of TMDs designed for 7-story building.

TMD Scenarios			$K_{di}(kN/mm)$	$C_{di}(kN.s/mm)$	$W_i(kN)$	μ_i	details
STMD	STMD Fund-T		2.939	0.098	680.4	0.03	Three STMD scenarios with 3% mass ratio each
	STMD N-L T1		1.075	0.059	680.4	0.03	
	STMD N-L T2		0.609	0.045	680.4	0.03	
MTMD	1st TMD	TMD Fund-T	1.008	0.020	226.8	0.01	One MTMD scenario with a total 3% mass ratio; each carry 1% mass ratio
	2nd TMD	TMD N-L T1	0.379	0.012	226.8	0.01	
	3rd TMD	TMD N-L T2	0.215	0.009	226.8	0.01	

To optimize control of the first dominant mode, each TMD scenario, will be placed atop the building, where the first mode exhibits the maximum amplitude. The controlled models are visually represented in **Figure 5**, showcasing the installation of STMD and MTMDs.

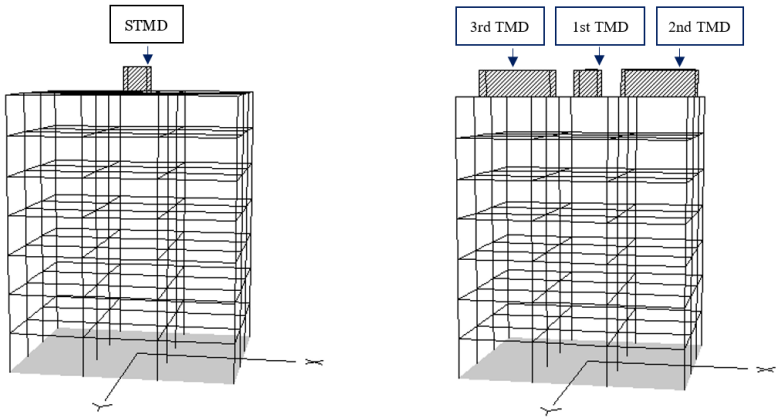

(a) Model wit STMD **(b)** Model wit MTMD

Figure 5. 7-story controlled frame models.

5.2. Seismic response

Following the dynamic nonlinear analysis of the building against four GMRs detailed in Section 4, a comprehensive assessment of maximum displacements is conducted across various scenarios. These scenarios include cases non-controlled (without TMD), with STMD tuned to the fundamental period (STMD-Fund T), STMD tuned to the time period corresponding to the second segment of the idealized trilinear (STMD N-L T1), STMD tuned to the time period corresponding to the third segment of the idealized trilinear (STMD N-L T2), and MTMDs with each tuned to time periods corresponding to three different segments of the idealized trilinear. The graphical representation of the maximum floor displacement for each of these distinct scenarios is presented in **Figure 6**.

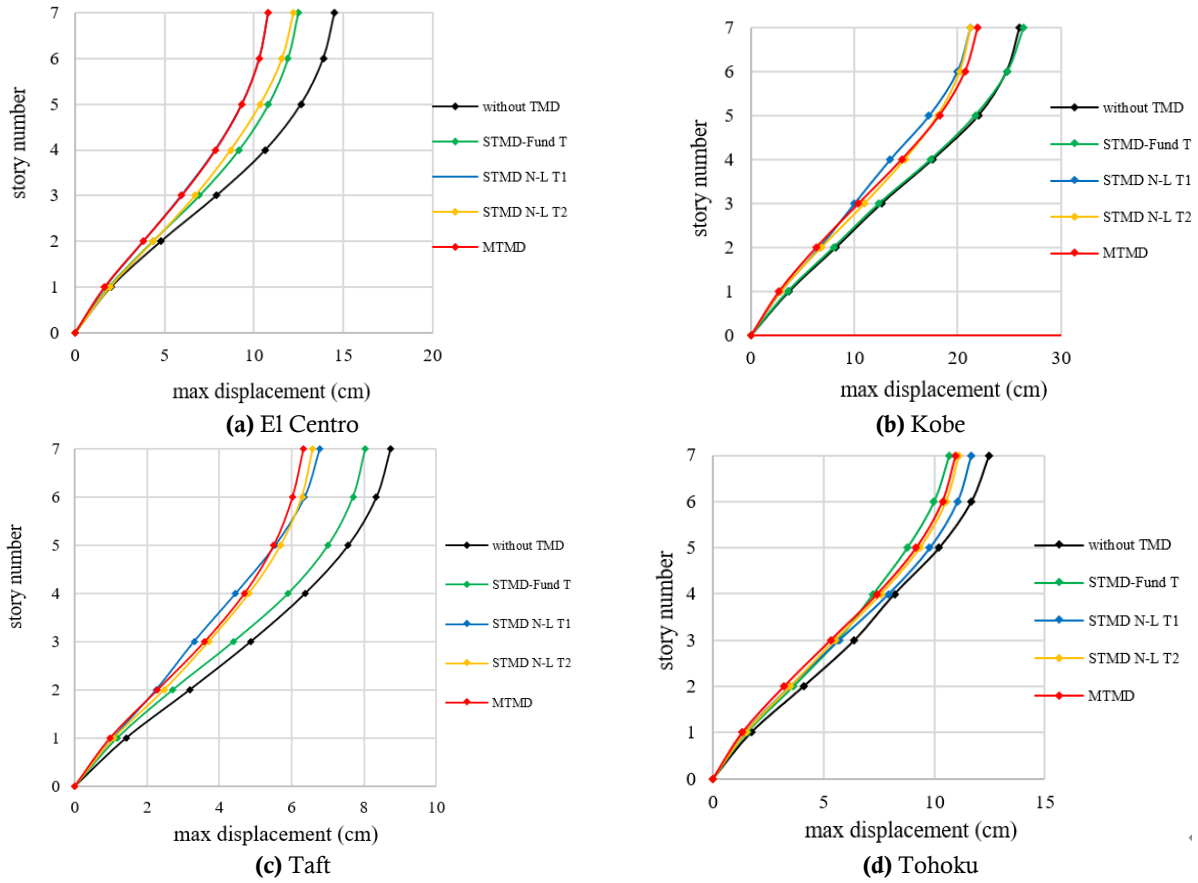

Figure 6. Maximum displacement response of 7-story building against.

As depicted in **Figure 6**, the conventional "STMD-Fund T" demonstrates a relatively modest reduction in maximum floor displacement across three earthquake records, with the exception of the Tohoku earthquake where it exhibits slightly improved performance compared to other scenarios. In this particular case, the difference is minimal, showcasing a 14.6% reduction in the maximum displacement of the top floor, compared to a 13.3% reduction in the MTMDs scenario. Notably, among the three STMD scenarios, "STMD N-L T1" and "STMD N-L T2" generally outperforms "STMD-Fund T", except in the case of the Tohoku earthquake. In a comprehensive comparison, MTMDs consistently demonstrate higher effectiveness than STMD scenarios, apart from the Kobe earthquake where "STMD N-L T1" exhibits a slight advantage. The MTMDs has effectively reduced the maximum displacement of the top floor by 25.8%, 15.4%, 27.6%, and 12.1% under the influence of the El Centro, Kobe, Taft, and Tohoku earthquakes, respectively. In contrast, the corresponding reductions for the "STMD-Fund T" are 14.1%, −1.5%, 7.9%, and 14.6%, following the same order.

Apart from assessing maximum floor displacements, the peak floor acceleration response is also regarded as a crucial performance objective for comparison. As illustrated in **Figure 7**, STMD scenarios exhibit nearly identical performance. Nevertheless, the MTMD scenario surpasses the STMD scenarios overall, except for the 6th floor against Taft and the 5th and 6th floors against Tohoku, where "STMD-Fund T" demonstrates a slightly better performance.

To visualize the temporal evolution of acceleration, **Figure 8** presents the acceleration time history experienced by the top floor during the El Centro earthquake. The findings for the Kobe, Taft, and Tohoku earthquakes are outlined in **Figures 9–11**, respectively. This dual evaluation offers a

comprehensive insight into the structural performance, under diverse seismic records.

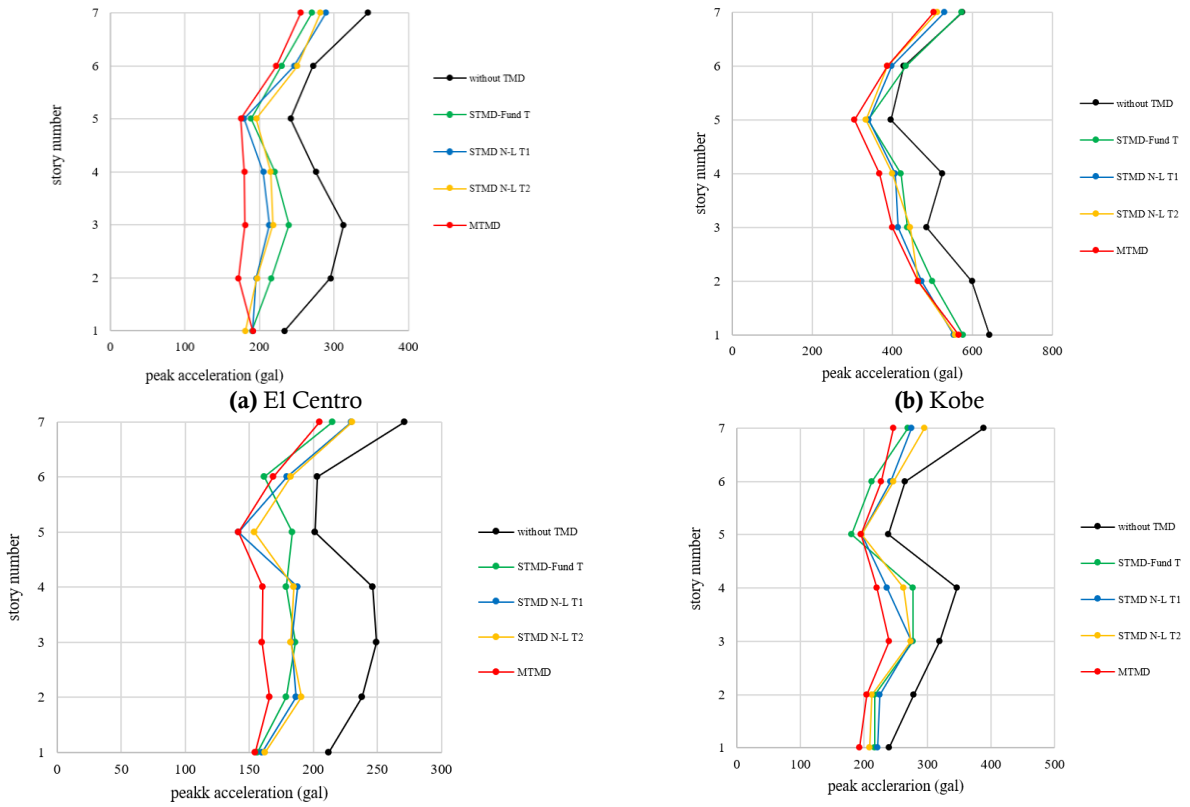

(a) El Centro **(b)** Kobe

(c) Taft **(d)** Tohoku

Figure 7. Peak floor acceleration response of 7-story building against.

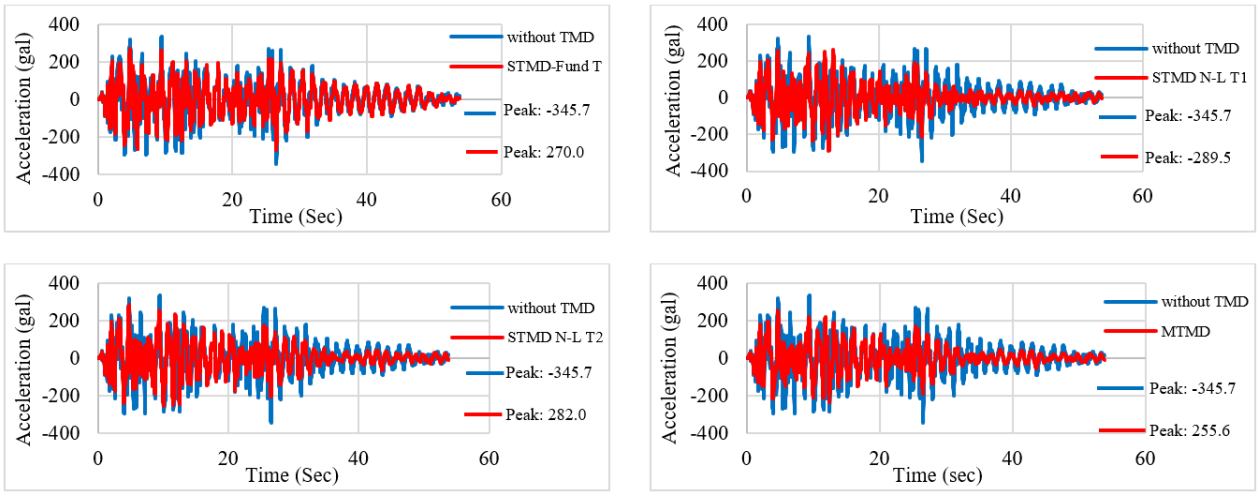

Figure 8. Top floor acceleration time history of non-controlled and controlled 7-story building with different TMD scenarios against El Centro.

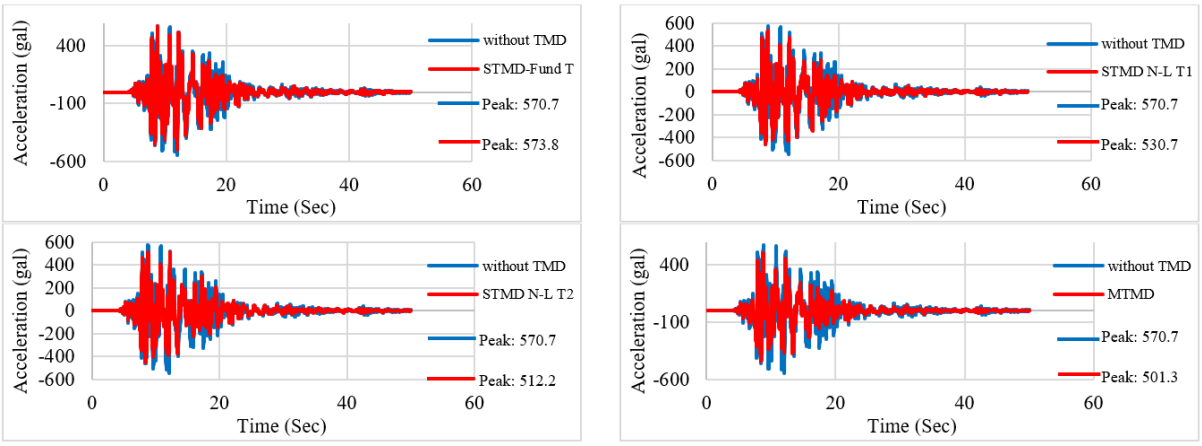

Figure 9. Top floor acceleration time history of non-controlled and controlled 7-story building with different TMD scenarios against Kobe.

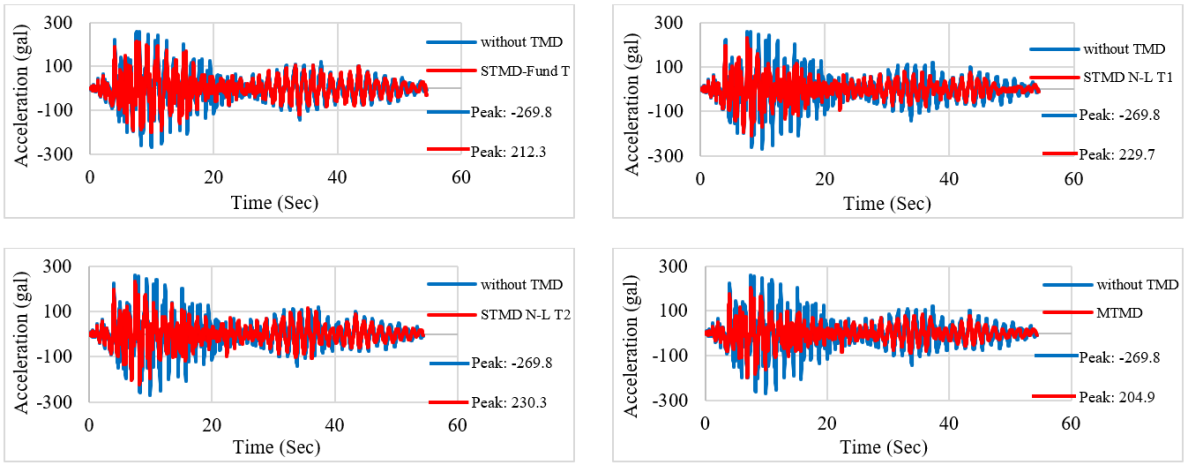

Figure 10. Top floor acceleration time history of non-controlled and controlled 7-story building with different TMD scenarios against Taft.

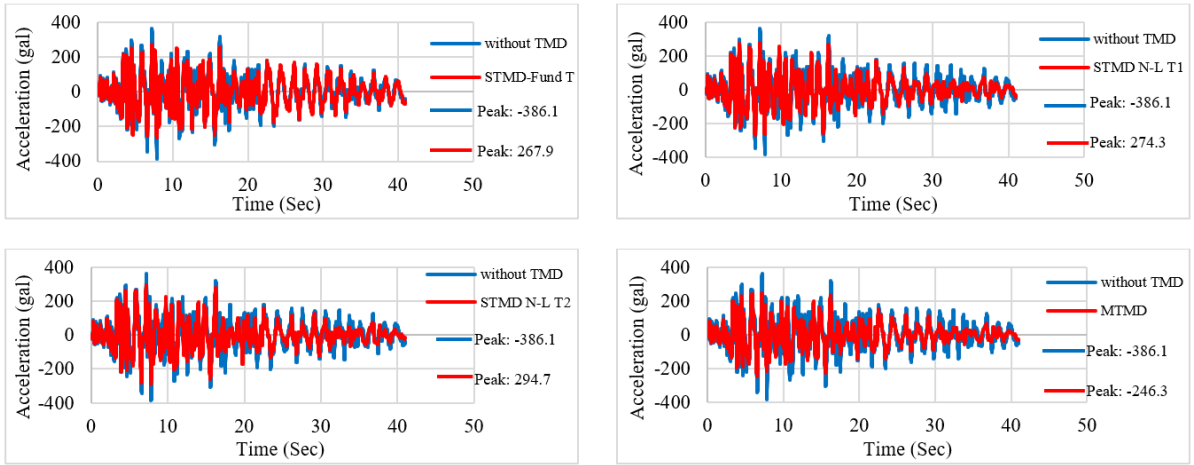

Figure 11. Top floor acceleration time history of non-controlled and controlled 7-story building with different TMD scenarios against Tohoku.

Upon observing the plotted results, it is evident that MTMDs overall outperform STMD scenarios, leading to a substantial reduction in the top-floor acceleration during the El Centro earthquake, as illustrated in Fig. 8. MTMDs resulted in a 26.1% reduction in peak acceleration, followed by the "STMD-Fund T" scenario with 21.9%, "STMD N-L T1" with 16.3%, and "STMD N-L T2" with 18.4%. Among

the STMD scenarios, while the peak acceleration values indicate the efficacy of "STMD-Fund T," an observing visually of acceleration time histories reveals the overall effectiveness of the other two STMD scenarios. This effectiveness hierarchy holds true across three additional earthquake records, emphasizing the significance of considering the nonlinear characteristics of the building in the TMD tuning process, as demonstrated in **Figures 9–11**.

6. Numerical Example 2 (25-story building)

6.1. Building information and TMD design

In addition to the 7-story RC building, the investigation extends to a 25-story RC building, portrayed in both its 3D frame model and plan in **Figure 12**. The assumed load weight per unit is set at 12 kN/m^2, resulting in a calculated weight of 4.536×10^3 kN for each story. The initial story stands at a height of 4200 mm, while the subsequent upper stories maintain a typical height of 3800 mm. Additionally, the fundamental damping ratio of the building is 0.02.

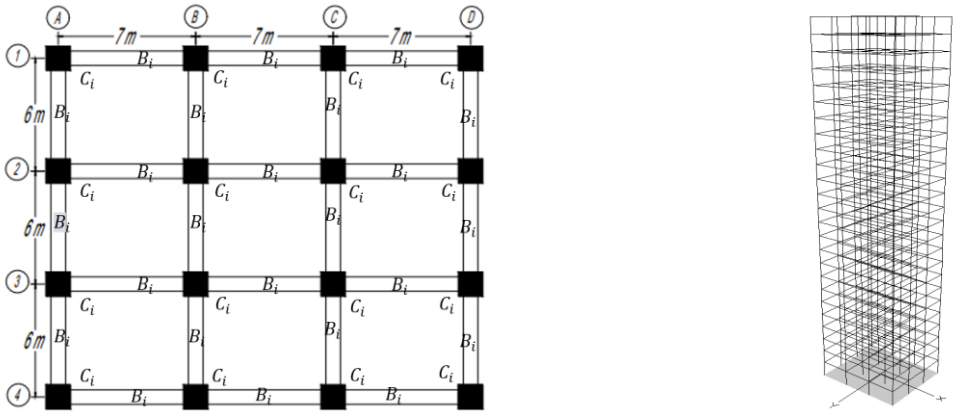

(a) Typical plan **(b)** Frame model

Figure 12. 25-Story model.

To gain a thorough insight into the building's structural elements, **Table 6** provides detailed information regarding the columns and beams.

Through pushover analysis of the non-controlled model, the resultant pushover capacity curve is illustrated in **Figure 13**. As detailed in the Section 2, the capacity curve is idealized by a trilinear representation.

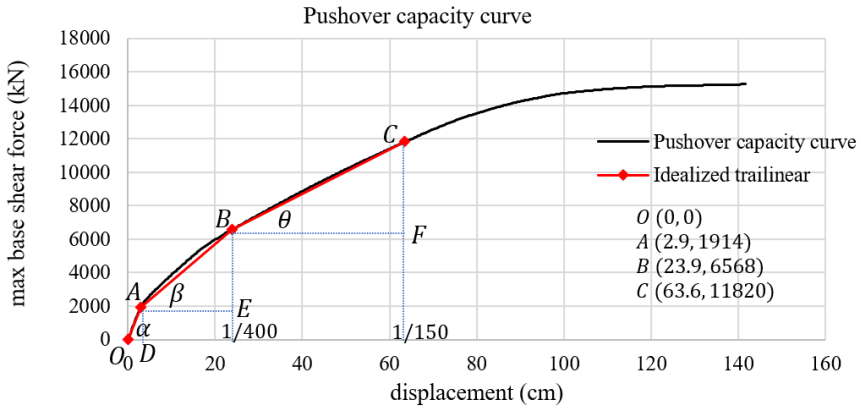

Figure 13. Illustration of Idealized trilinear on pushover capacity curve of 25-story building in the X-direction.

Table 6. Element properties of 25-story building.

Floors	Members	dimensions(mm)	Longitudinal rebars		$F_c(N/mm^2)$	$F_y(N/mm^2)$
1	C_1	900 × 900	24Ø35		34	390
2–5	C_2	900 × 900	20Ø35		34	390
6–10	C_3	850 × 850	20Ø35		34	390
11–14	C_4	850 × 850	16Ø35		34	390
15–19	C_6	750 × 750	20Ø32		34	390
20–22	C_7	750 × 750	16Ø32		34	390
23–55	C_8	750 × 750	16Ø29		34	390
1–5	B_1	b = 600, h = 850	Top	8Ø32	34	390
			Bottom	8Ø32		
6–10	B_2	b = 550, h = 800	Top	8Ø32	34	390
			Bottom	8Ø32		
11–14	B_3	b = 550, h = 750	Top	7Ø32	34	390
			Bottom	7Ø32		
15–19	B_4	b = 500, h = 750	Top	7Ø29	34	390
			Bottom	7Ø29		
20–23	B_5	b = 500, h = 750	Top	6Ø29	34	390
			Bottom	6Ø29		
23–25	B_6	b = 500, h = 700	Top	6Ø29	34	390
			Bottom	6Ø29		

By performing eigenvalue analysis of non-controlled building, the mode shape corresponding to the first dominant mode was obtained. Utilizing Equation (1), the effective mass of the first mode is computed to be 8.449 $kN.s^2/mm$. Considering **Figure 13**. and the calculated value of the effective mass for the first mode, the corresponding three time periods are computed, as presented in **Table 7**.

Table 7. Time periods corresponding to three segments of idealized trilinear pushover capacity curve of 25-story building.

angle	Stiffness(K)	$K_i(kN/cm)$	$T_i = 2\pi\sqrt{\frac{m_{eff}}{K_i}}$(sec)	Hereinafter referred as
$\tan\alpha$	$K_1 = \overline{AD}/\overline{OD}$	$K_1 = 650.6$	$T_1 = 2.264$	Fund T
$\tan\beta$	$K_2 = \overline{BE}/\overline{AE}$	$K_2 = 222.6$	$T_2 = 3.871$	$N - LT_1$
$\tan\theta$	$K_3 = \overline{CF}/\overline{BF}$	$K_3 = 132.1$	$T_3 = 5.025$	$N - LT_2$

Considering the decided mass ratio (in this case, 3%) and employing Equations (2)–(6), the stiffness and damping coefficients for each TMDs are computed, as outlined in **Table 8**.

To enhance the control of the first dominant mode, each TMD scenario, along with its calculated parameters, will be strategically positioned at the top of the building, precisely targeting the floor where the first mode demonstrates the maximum amplitude. The controlled frame models are visually depicted in **Figure 14**, illustrating the installation of STMD and MTMDs.

Table 8. Parameter values and information of TMDs designed for 25-story building.

TMD Scenarios			$K_{di}(kN/mm)$	$C_{di}(kN.s/mm)$	$W_i(kN)$	μ_i	Detail
STMD	STMD Fund-T		2.616	0.207	3402	0.03	Three STMD scenarios with 3% mass ratio each.
	STMD N-L T1		0.835	0.117	3402	0.03	
	STMD N-L T2		0.495	0.090	3402	0.03	
MTMD	1st TMD	TMD Fund-T	0.860	0.040	1134	0.01	One MTMD scenario with a total 3% mass ratio; each carry 1% mass ratio
	2nd TMD	TMD N-L T1	0.294	0.024	1134	0.01	
	3rd TMD	TMD N-L T2	0.175	0.018	1134	0.01	

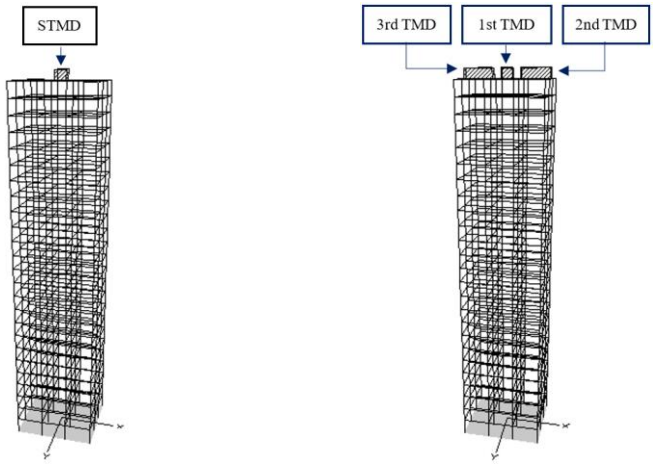

(a) Model wit STMD **(b)** Model wit MTMD

Figure 14. 25-story controlled frame models.

6.2. Seismic response

Similar to the 7-story building, dynamic nonlinear analysis was performed on the 25-story structure using four selected GMRs, as outlined in Section 4. A comprehensive assessment of maximum displacements was then performed across various scenarios, aligning with those discussed for the 7-story building in Section 5.

As depicted in **Figure 15**, "STMD-Fund T" shows the least reduction in maximum floor displacement compared to all other scenarios. The effectiveness, ranked from less effective to more effective, is followed by "STMD N-L T2" in the second position and "STMD N-L T1" in the third position. This emphasizes the importance of considering the middle segment of the idealized trilinear form in controlling tall non-linear buildings.

Furthermore, the MTMDs demonstrate robustness compared to all STMD scenarios except for the Kobe earthquake, where "STMD N-L T1" exhibits slightly superior performance only on the 17th to 22nd floors. The conventional STMD tuned to the fundamental period reduces the top floor's maximum displacement by about 3.7%, 5.9%, 12.1%, and 13.3% against El Centro, Kobe, Taft, and Tohoku, respectively. However, for MTMDs, these values in the same order are 11.1%, 22.1%, 25.1%, and 28.2%.

In addition to evaluating maximum floor displacements, the peak acceleration response is also considered as a vital performance objective for comparison. As the results are illustrated in **Figure 16**, it is evident that the STMD tuned to the time periods corresponding to the non-linearity of the building exhibited superior performance when compared to the conventional STMD tuned to the fundamental period. However, the MTMD configuration consistently outperformed all the STMD scenarios, with the

exception of the Taft earthquake, where "STMD N-L T2" demonstrated slightly better performance.

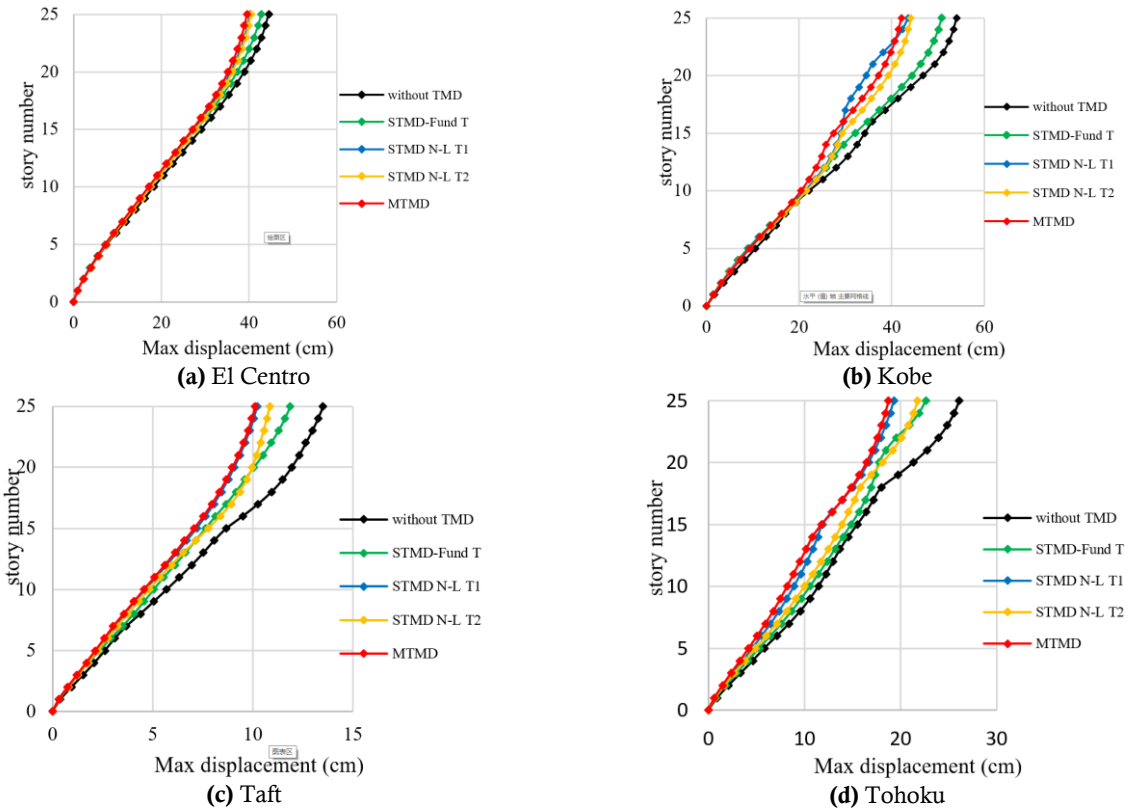

(a) El Centro **(b)** Kobe **(c)** Taft **(d)** Tohoku

Figure 15. Maximum displacement response of 25-story building against.

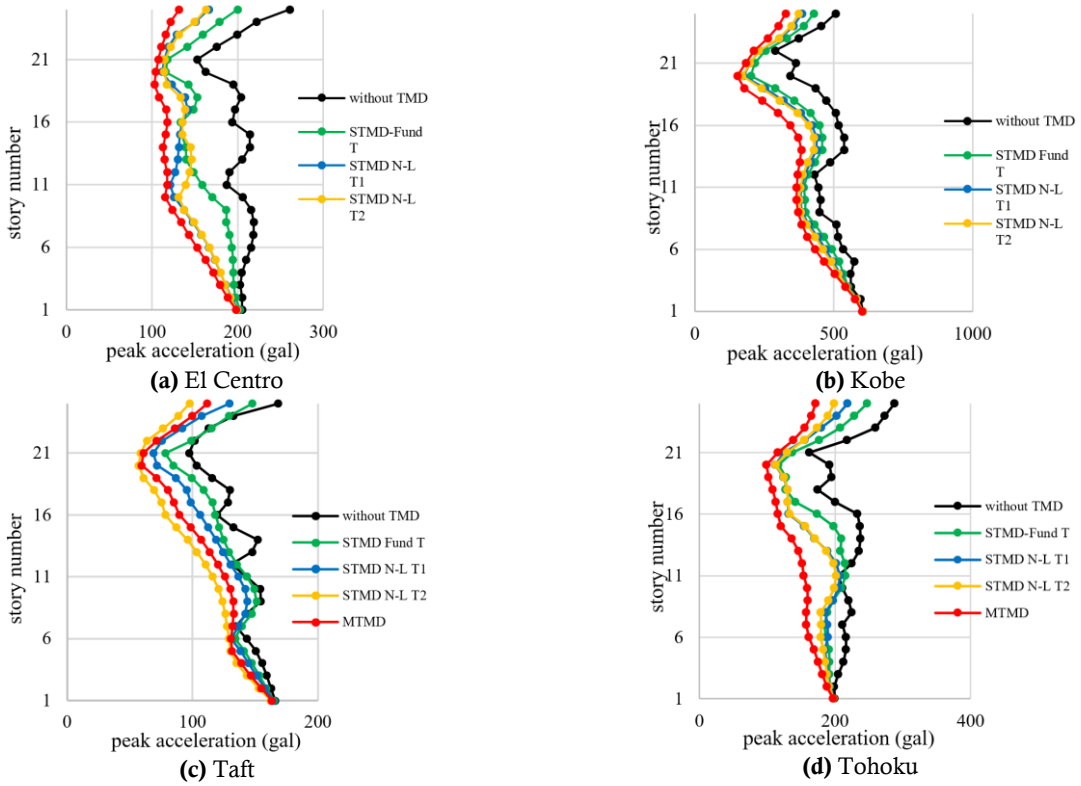

(a) El Centro **(b)** Kobe **(c)** Taft **(d)** Tohoku

Figure 16. Peak floor acceleration response of 25-story building against.

To depict the acceleration over time, **Figure 17** illustrates the acceleration time history of the top floor during the El Centro earthquake. The results for the Kobe, Taft, and Tohoku earthquakes are detailed in **Figures 18–20**, respectively.

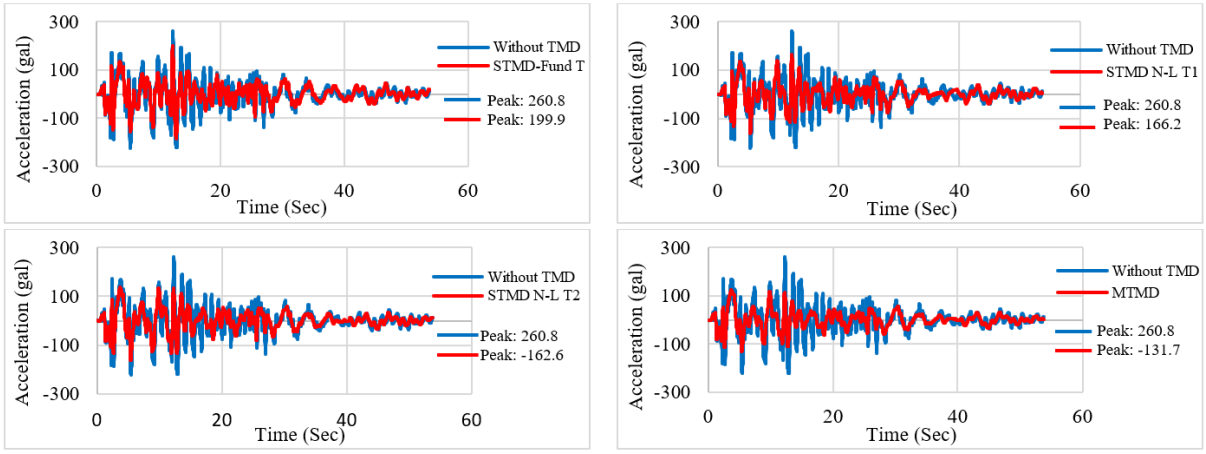

Figure 17. Top floor acceleration time history of non-controlled and controlled 25-story building with different TMD scenarios against El Centro.

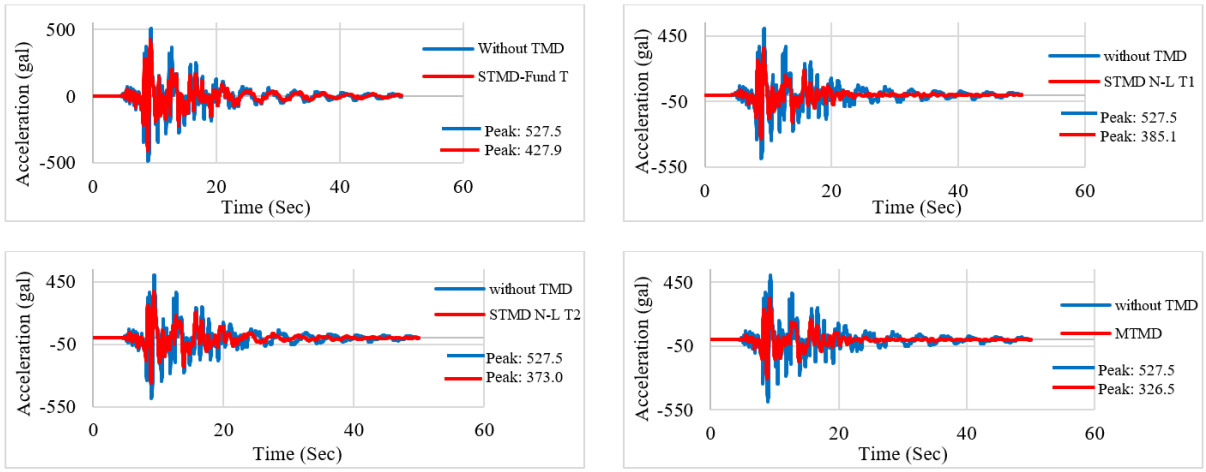

Figure 18. Top floor acceleration time history of non-controlled and controlled 25-story building with different TMD scenarios against Kobe.

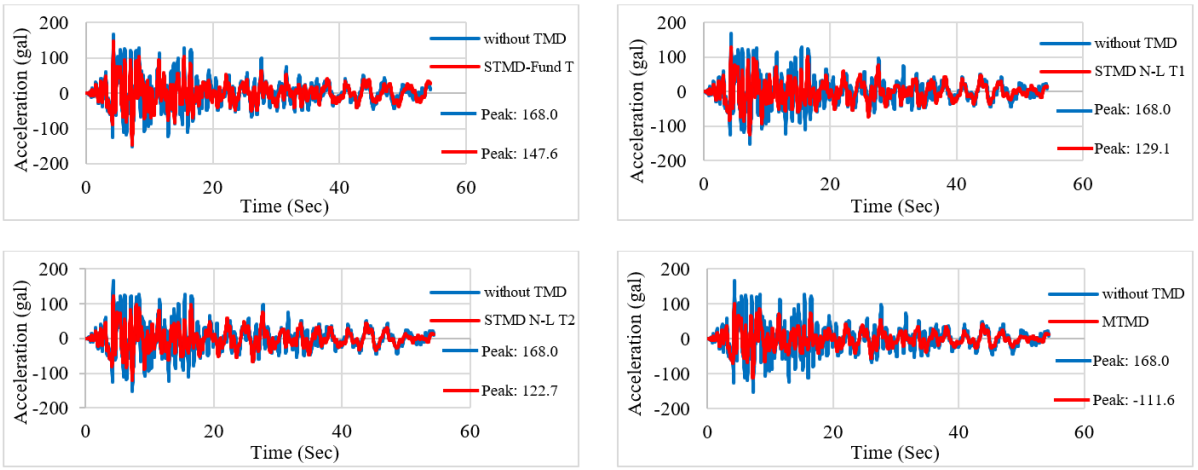

Figure 19. Top floor acceleration time history of non-controlled and controlled 25-story building with different TMD scenarios against Taft.

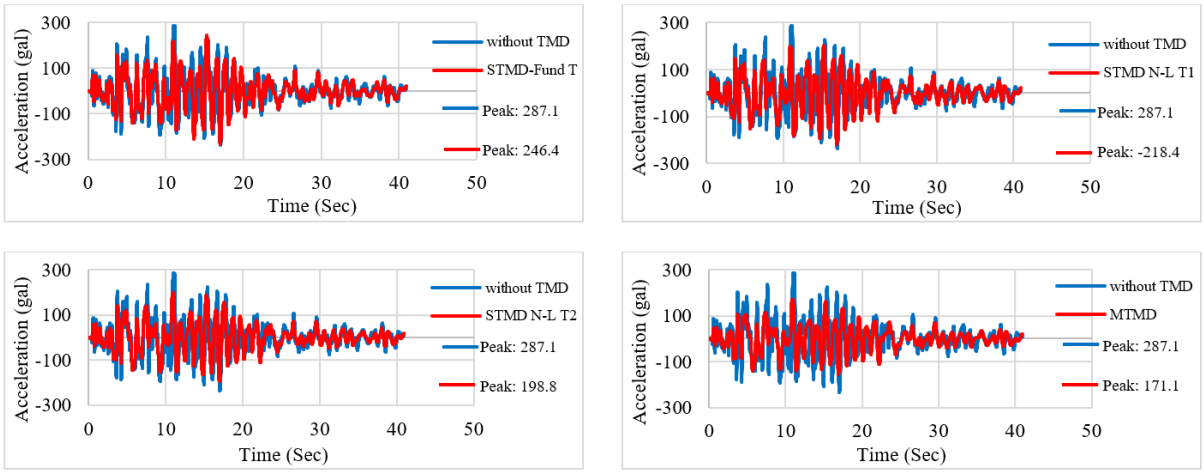

Figure 20. Top floor acceleration time history of non-controlled and controlled 25-story building with different TMD scenarios against Tohoku.

As demonstrated in **Figure 17**, the conventional "STMD Fund T" exhibited a comparatively smaller reduction in the acceleration of the top floor during the El Centro earthquake compared to other scenarios. The effectiveness increased with the installation of "STMD N-L T1," followed by "STMD N-L T2," and MTMDs demonstrated the highest level of robustness. The MTMD configuration achieved a significant reduction, approximately 49.5%, in peak acceleration against the El Centro earthquake. In contrast, the reductions for "STMD-Fund T," "STMD N-L T1," and "STMD N-L T2" are 23.4%, 36.3%, and 37.6%, respectively. In summary, MTMDs demonstrated higher effectiveness compared to all STMD scenarios. This order of effectiveness holds true for the three other earthquake records, as illustrated in **Figures 18–20**.

6.3. Wind response

Due to the sensitivity of tall structures to strong winds, only the previous 25-story building serves as the focus of wind load analysis. The models include the base case without TMD and three additional scenarios, incorporating STMD and MTMDs. The dynamic wind load is simulated using the NatHaz online wind simulator[14,17], generating wind velocity time history. This analysis assumes that gust wind speed is 50 m/s, and the building is situated in an area categorized as exposure category C (open terrain with scattered obstructions having heights generally less than 30 feet (9.14 m); according ASCE 7–10). Subsequently, the wind force time history at each floor level is computed by applying Bernoulli's theorem.

$$F_i(t) = 0.5\rho C_d A_i [U_i + u_i(t)]^2 \quad (7)$$

where ρ is the density of air; C_d is the drag coefficient; A_i is tributary area of the i^{th} floor; U_i and $u_i(t)$ are the mean wind speed and the fluctuating wind speed at the i^{th} floor, respectively. For this study $\rho = 1.2\ {}^{kg}/_{m^3}$ and C_d is set to 1.3 based on the rectangular shape of the building[18]. Using the Equation (7), the wind force time history of the 24^{th} story is generated as shown in **Figure 21**.

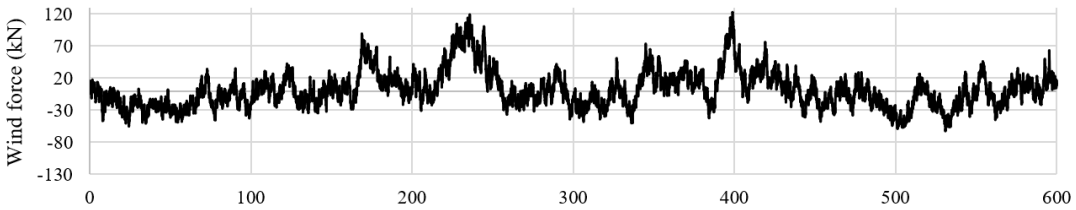

Figure 21. Wind load time history for the 24th story of 25-story building.

Considering the decided mass ratio (3%), and applying Equations (2)–(6), the stiffness and damping coefficients for each TMD are computed and presented in **Table 9**. Given that the wind load is comparatively less formidable than seismic loads, the building's stiffness is not expected to undergo a significant reduction. For example, in the context of the 25-story building under study, the base shear acting on the non-controlled structure is $3.005 \times 10^3\ kN$ due to wind load. Consequently, the third segment of the idealized trilinear is disregarded in this analysis.

Table 9. Parameter values and information of TMDs designed for 25-story building-wind excitation.

TMD Scenarios		$K_{di}(kN/mm)$	$C_{di}(kN.s/mm)$	$W_i(kN)$	μ_i
STMD	STMD Fund-T	2.616	0.207	3402	0.03
	STMD N-L T	0.835	0.117	3402	0.03
MTMD	TMD Fund-T	1.364	0.076	1701	0.015
	TMD N-L T	0.852	0.060	1701	0.015

The wind load time history generated is applied along the height of the building using a distribution pattern that takes into account the ratio of wind force at each floor for the analysis. The results of the analysis, considering the maximum floor displacement and peak acceleration as performance objectives, are illustrated in **Figure 22**.

As illustrated in Figure 22a, both "STMD N-L T" and MTMD demonstrate closely aligned outcomes in minimizing maximum floor displacement, with a slight performance advantage observed for "STMD N-L T" over MTMD. In contrast, the STMD tuned to the fundamental period of the building demonstrates less effectiveness compared to the other two scenarios. The reduction in the maximum displacement of the top floor is 24.8%, 37.0%, and 33.1% for "STMD-Fund T," "STMD N-L T," and MTMD, respectively.

The peak floor acceleration is also considered as another performance objective and the result of analysis presented in Figure 22b. Both scenarios of STMD exhibit comparable performance, with minor variations observed on specific floors. Notably, in the initial four floors, "STMD-Fund T" demonstrates superior performance, while on the 5th and 6th floors, "STMD N-L" outperforms. Upon conducting a comprehensive comparison, it is evident that MTMD outperforms STMD from the ground floor up to the 19th floor. However, it is worth mentioning that STMD scenarios marginally outperform MTMD on the top six floors.

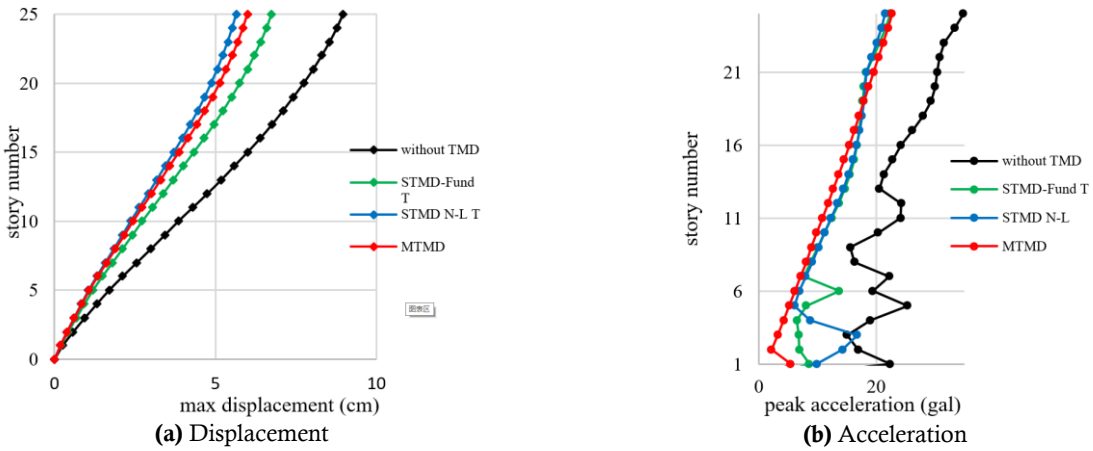

(a) Displacement **(b)** Acceleration

Figure 22. Response of the 25-story building against wind excitation.

To visualize the temporal evolution of acceleration, **Figure 23** portrays the time history of acceleration experienced by the top floor against wind excitation.

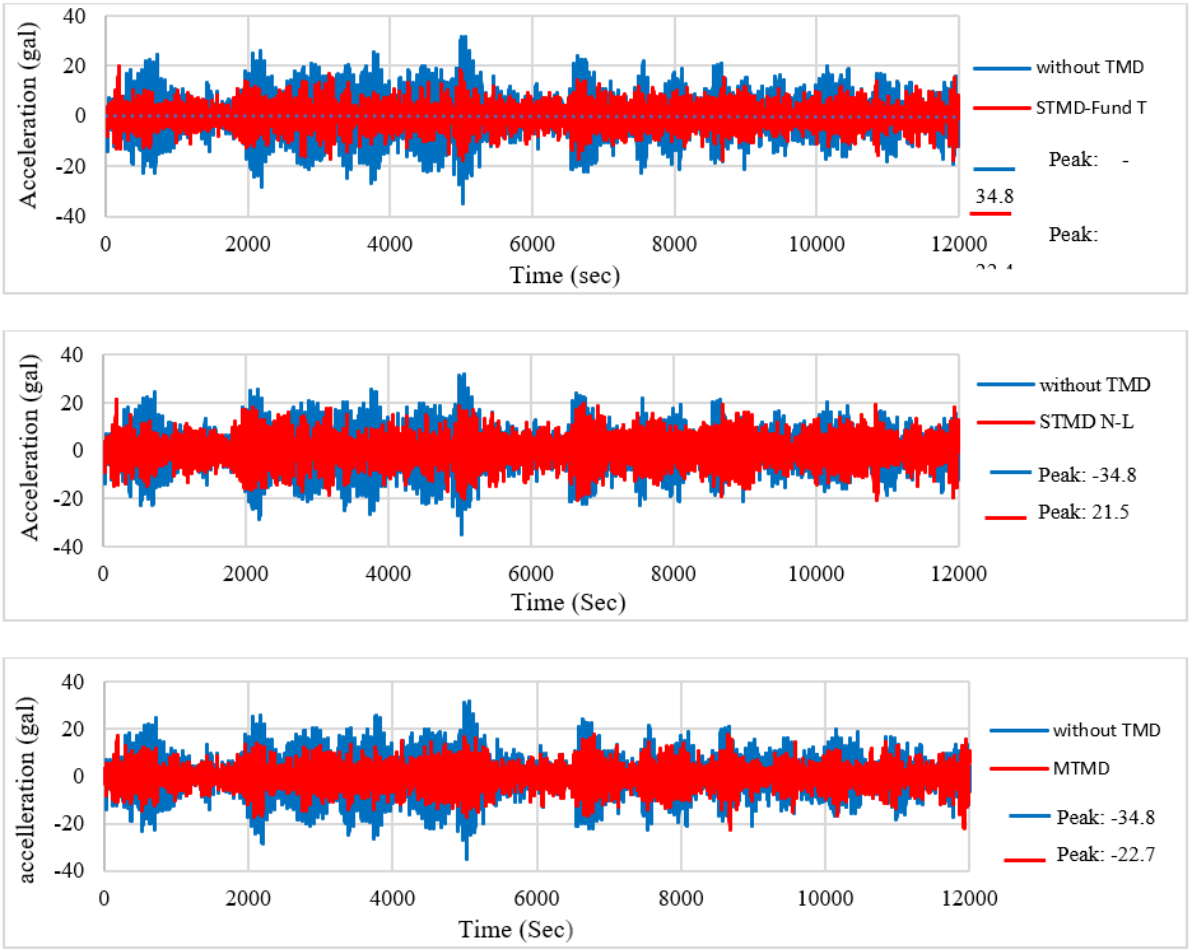

Figure 23. Top floor acceleration time history of the 25-story building subjected to wind load.

Examining **Figure 23**, within the STMD category, the effectiveness of scenarios demonstrates a noticeable trend from less effective to more effective, with "STMD-Fund T" and "STMD N-L T" arranged in ascending order of effectiveness. The recorded reduction in peak acceleration values for these two STMD scenarios are 35.6% and 38.2%, respectively, while the corresponding value for the MTMD scenario is 34.8%.

In summary, the study emphasizes the importance of considering stiffness degradation due to nonlinear behavior when designing TMD for addressing building nonlinearity. Results altogether highlight the robustness of STMDs tuned to time periods corresponding to nonlinearity segments compared to conventional STMDs under dynamic loads, especially in tall building. Notably, MTMD each tuned to three distinct time periods aligned with trilinear segments, demonstrate even greater robustness than any STMD scenario. These findings provide valuable insights for seismic retrofitting and structural dynamics, positioning MTMDs as a compelling solution to minimize maximum floor displacement and acceleration, enhancing overall building dynamic performance.

7. Conclusions

In conclusion, this study introduces a novel control strategy for addressing non-linear building

behavior by precisely tuning TMDs to specific time periods following non-linearity onset. The proposed methodology incorporates pushover analysis to establish the pushover capacity curve. Subsequently, this curve is represented by an idealized trilinear form, characterized by key points at the origin, nonlinearity onset, and positions corresponding to target drifts (1/400 and 1/150). This representation facilitates the calculation of time periods for each segment of the trilinear, enabling the precise tuning of TMDs to match these specific time periods. The proposed approach, represents a significant advancement in enhancing building performance under non-linear conditions.

The research underscores the critical importance of tuning TMDs to specific time periods corresponding to the non-linear behavior zone. STMDs tuned to these periods exhibit remarkable robustness, surpassing the performance of conventional STMDs tuned to the fundamental period. Moreover, MTMDs tuned to three distinct time periods demonstrate superior robustness compared to all STMD scenarios, particularly in minimizing maximum floor displacement and acceleration of tall buildings under seismic loads.

Furthermore, wind load analysis reveals the effectiveness of TMD scenarios, with both MTMDs and STMDs tuned to time periods corresponding to non-linearity region outperforming conventional STMDs tuned to the fundamental period. This study not only establishes the effectiveness of the proposed strategy but also positions MTMDs as a compelling solution, showcasing their robustness in minimizing both maximum floor displacement and acceleration.

In summary, the strategy of tuning TMDs to specific time periods following non-linearity onset proves effective in enhancing building performance under non-linear conditions. The findings from this study suggest a valuable framework for improving the seismic and wind resilience of tall buildings.

Author contributions

Conceptualization, TS and HA; methodology, TS and HA; software, TS; validation, TS; formal analysis, HA; investigation, HA; resources, TS and HA; data curation, HA; writing—original draft preparation, HA; writing—review and editing, HA; visualization, HA; supervision, TS; project administration, TS. All authors have read and agreed to the published version of the manuscript.

Conflict of interest

The authors declare no conflict of interest.

References

1. Boccamazzo A, Carboni B, Quaranta G, et al. Seismic effectiveness of hysteretic tuned mass dampers for inelastic structures. Engineering Structures. 2020, 216: 110591. doi: 10.1016/j.engstruct.2020.110591
2. Huang H, Mosalam KM, Chang WS. Adaptive tuned mass damper with shape memory alloy for seismic application. Engineering Structures. 2020, 223: 111171. doi: 10.1016/j.engstruct.2020.111171
3. Lu Z, Chen X, Zhang D, et al. Experimental and analytical study on the performance of particle tuned mass dampers under seismic excitation. Earthquake Engineering & Structural Dynamics. 2016, 46(5): 697-714. doi: 10.1002/eqe.2826
4. Elias S, Matsagar V. Seismic vulnerability of a non-linear building with distributed multiple tuned vibration absorbers. Structure and Infrastructure Engineering. 2019, 15(8): 1103-1118. doi: 10.1080/15732479.2019.1602149
5. Domizio M, Garrido H, Ambrosini D. Single and multiple TMD optimization to control seismic response of nonlinear structures. Engineering Structures. 2022, 252: 113667. doi: 10.1016/j.engstruct.2021.113667
6. Mohebbi M, Joghataie A. Designing optimal tuned mass dampers for nonlinear frames by distributed genetic algorithms. The Structural Design of Tall and Special Buildings. 2011, 21(1): 57-76. doi: 10.1002/tal.702
7. Shamsaddinlou A, Shirgir S, Hadidi A, et al. An efficient reliability-based design of TMD & MTMD in

nonlinear structures under uncertainty. Structures. 2023, 51: 258-274. doi: 10.1016/j.istruc.2023.03.053
8. Sgobba S, Marano GC. Optimum design of linear tuned mass dampers for structures with nonlinear behaviour. Mechanical Systems and Signal Processing. 2010, 24(6): 1739-1755. doi: 10.1016/j.ymssp.2010.01.009
9. Roozbahan M, Jahani E. Optimal design of elastic and elastoplastic tuned mass dampers using the Mouth Brooding Fish algorithm for linear and nonlinear structures. Structures. 2022, 43: 1084-1090. doi: 10.1016/j.istruc.2022.07.037
10. Structural Earthquake Response Analysis Software, STERA-3D Version 11.4. Available online: http://www.rc.ace.tut.ac.jp/saito/software-e.html (accessed on 22 December 2023).
11. Saito T. STERA-3D Technical Manual. Version 7.2, TUT, Japan.
12. Tsai H, Lin G. Optimum tuned-mass dampers for minimizing steady-state response of support-excited and damped systems. Earthquake Engineering & Structural Dynamics. 1993, 22(11): 957-973. doi: 10.1002/eqe.4290221104
13. Conner JJ. Introduction to Structural Motion Control (Chapter 4: 217-285). Pearson Education, Inc; 2003.
14. Global component of the center for engineering strong motion data. Strong-motion virtual data center. Available online: https://www.strongmotioncenter.org/vdc/scripts/search.plx (accessed on 22 December 2023).
15. National center for environmental information. NOAA. Available online: https://www.ngdc.noaa.gov/hazel/view/hazards/earthquake/search (accessed on 22 December 2023).
16. ViewWave Software Version 2.2.6. Kashima's Office. Available online: https://smo.kenken.go.jp/~kashima/viewwave/download (accessed on 22 December 2023).
17. NatHaz on-line wind simulator (NOWS). Available online: http://windsim.ce.nd.edu/gew_init2.html (accessed on 22 December 2023).
18. Banerjee S, Ghosh AD, Matsagar VA. Optimum design of nonlinear tuned mass damper for dynamic response control under earthquake and wind excitation. Struct Control Heal Monit. 2022, 29(7). doi: 10.1002/stc.2960